# Impact of Temperature on Nonlinearity of Voltage Transformers in Harmonics Measurement

# Impact of Temperature on Nonlinearity of Voltage Transformers in Harmonics Measurement

Palma Sara Letizia, Gabriella Crotti, Antonio Delle Femine, *Member, IEEE*, Daniele Gallo, *Member, IEEE*, Claudio Iodice, *Student Member, IEEE*, Carmine Landi, *Senior Member, IEEE*, Mario Luiso, *Member, IEEE*, Davide Signorino, and Domenico Giordano, *Member, IEEE*

***Abstract*—The aim of the study here presented is to evaluate how temperature variations affect the metrological performance of inductive voltage transformers (VTs) in harmonic measurements. The analysis specifically targets the harmonics up to 1 kHz, where measurements using VTs can be challenging due to their nonlinear behavior. In fact, recent scientific literature has evidenced that when a VT operates under distorted conditions, the harmonics at its secondary side are not simply a scaled version of those injected. Instead, they are a combination of the injected harmonics and the spurious ones generated by the iron core due to its *B*–*H* curve. This phenomenon has been investigated in laboratory under controlled conditions, and the specific techniques have been proposed to compensate for it. However, no studies have analyzed the impact of temperature variation on this phenomenon and, consequently, on the introduced errors. This article addresses this open issue through experimental activities on two different VTs using a high-accuracy reference setup. Results show that, for different temperatures, the measured VT harmonic errors can differ up to an order of magnitude, indicating that this influence quantity cannot be neglected.**

***Index Terms*—Harmonics measurement, instrument transformers (ITs), power system measurement, temperature variation.**

## I. Introduction

HARMONICS represent one of the most critical power quality (PQ) phenomena due to their increase in recent years and the associated issues. Harmonics are injected into distribution grids by newly and widely installed devices essential for achieving net zero emissions and reducing dependence on fossil fuel [1], [2].

In fact, the primary contributors to harmonic distortion are switching-type power converters extensively used in renewable energy parks, electric vehicle (EV) chargers, energy storage facilities, and high-voltage direct current (HVdc) systems [3].

Received 10 October 2024; revised 16 January 2025; accepted 4 February 2025. Date of publication 6 March 2025; date of current version 26 March 2025. This work was supported by European Partnership on Metrology (EPM) under e-Treny and ADMIT Projects through European Union's Horizon Europe Research and Innovation Program and Participating States under Project 22NRM04 and Project 22NRM06. The Associate Editor coordinating the review process was Dr. D. Slomovitz. *(Corresponding author: Palma Sara Letizia.)*

Palma Sara Letizia, Gabriella Crotti, Davide Signorino, and Domenico Giordano are with the Divisione Metrologia dei materiali innovativi e scienze della vita, Istituto Nazionale di Ricerca Metrologica, 10135 Turin, Italy (e-mail: p.letizia@inrim.it).

Antonio Delle Femine, Daniele Gallo, Claudio Iodice, Carmine Landi, and Mario Luiso are with the Dipartimento di Ingegneria, Università degli Studi della Campania "Luigi Vanvitelli," 81031 Aversa, Italy (e-mail: mario.luiso@unicampania.it).

Digital Object Identifier 10.1109/TIM.2025.3548764

Harmonic distortion in supply voltage presents several problems, such as overheating of the neutral conductor in three-phase systems, increased losses in transformers due to skin effect and eddy currents, and elevated temperatures in motors and transformers, reducing efficiency and lifespan of the entire grid.

In this scenario, it is necessary to have an accurate monitoring of harmonics and more in general PQ phenomena [4]. In medium-voltage (MV) grids, the PQ measurement chain always includes transducers to scale down voltage and current to levels fitting with a low-voltage (LV) PQ analyzer. This task is commonly assigned to inductive instrument transformers (ITs) that are already installed in MV grids for metering and protection applications. As a consequence, it is clear that the ITs frequency performance has a significant impact on the overall accuracy associated with the measurement of harmonics and PQ in general. The recently released standard IEC 61869-1 edition 2 [5] introduces extensions to the accuracy classes of ITs in frequency up to 500 kHz. However, it lacks guidance on measurement methodologies, testing procedures, reference instrumentation, or uncertainty evaluation at frequency different from the power one. Additionally, while the standard [5] requires accuracy verification for low-power ITs (LPITs) up to the 13th harmonic, it excludes inductive ITs, which are covered in the existing standards [6], [7] only in terms of accuracy and characterization at power frequency.

On the other hand, scientific literature has faced the topic of inductive ITs used in harmonic and PQ measurement in last decades [8], [9] and highlighted the necessity of defining proper test procedure for their accurate frequency characterization [10]. In this respect, the review articles [11], [12] provide a deep analysis of many papers proposing methods, setup, and test conditions for the evaluation of ITs accuracy in the measurement of distorted test waveforms at LV and MV levels. However, in literature, the issue of using IT for PQ measurements has also been evidenced focusing on transmission systems operating at hundreds of kilovolts [13], and proper generation and measurement setup for their characterization have been designed and developed in some National Metrology Institutes (NMIs) [14]. In recent years, the behavior of ITs has also been investigated at frequencies higher than those typically associated with harmonic monitoring [15], [16].

Considering inductive voltage transformer (VT), scientific literature has highlighted two important issues regarding their frequency behavior, which can limit their utility in harmonics monitoring: 1) nonlinearity associated with the measurement of first 10–15 harmonics and 2) resonance phenomenon. Regarding the first issue, Cataliotti et al. [17], Kaczmarek and Stano [18], and Toscani et al. [19] have shown that VTs can introduce the errors of some percent in the measurement of harmonics because of the $B$–$H$ curve of their iron core. In fact, when a VT is supplied with a pure sinusoidal waveform at rated amplitude and frequency, it produces an output voltage composed not only of the scaled fundamental tone but it also includes other spurious harmonic tones up to some hundreds of hertz. Consequently, when the VT is supplied with a voltage composed of a fundamental tone plus superimposed harmonic tones, the harmonics observed at the output side will be the combination of the injected and the spurious ones. This phenomenon leads to measurement errors, as the secondary harmonics are not just a scaled representation of the primary ones. The VT resonance phenomenon can be explained considering that the electrical model of a VT includes both inductance and stray capacitance [20]. Depending on the rated primary voltage, the first resonance can occur at few kHz and, in the presence of the resonance, the errors introduced by the VT in the frequency measurement can reach hundreds of percentage [21]. Regarding the VT resonance phenomenon, it has been shown to depend on the operating temperature of the VT; specifically, as the temperature increases, both the frequency of the first resonance and the maximum error decrease [22]. More generally, it has been evidenced that other influencing factors, such as burden conditions, and their combinations [23], [24], [25] can affect the VT frequency performance.

As the nonlinearity error of VTs in measuring harmonics, the existing literature only focuses on the proposal, validation [17], [19], and comparison [26] of various compensation techniques aimed at significantly reducing it. All proposed compensation techniques have been studied and validated under constant and controlled temperature conditions. They involve a laboratory identification step to determine a compensation lookup table to be applied to the on-site measured harmonics. However, the study of the impact of possible influencing quantities on nonlinearities, and thus on the validity of techniques for their compensation, has not been explored. In this context, the study presented in this article aims to investigate the influence of temperature on the nonlinear behavior of VTs and, consequently, on the related effect on the ratio error and phase displacement when measuring harmonics. To achieve this goal, the setup typically adopted for the frequency characterization of MV VTs under realistic conditions, but controlled laboratory conditions have been modified to include a climatic chamber and two commercial VTs, one for indoor application and one for the outdoor one, are tested.

This article is organized as follows. Section II provides a brief overview related to the standard covering both ITs and electrical substations range of variation of temperature. In Section III, the theoretical background on the phenomenon of VTs nonlinearity is recalled. Section IV described the experimental setup and test procedure adopted to assess the impact of temperature on the VT nonlinearity. Section V presents the experimental results, and in Section VI, a discussion of experimental tests is provided. Finally, Section VII draws the conclusion.

TABLE I
ITs Operating Ambient Temperature Categories According to IEC 61869-1 Standard

| Class | Lowest temperature in °C | Highest temperature in °C |
|---|---|---|
| -5/40 | -5 | 40 |
| -25/40 | -25 | 40 |
| -40/40 | -40 | 40 |

## II. Review of In-Force Standards

This section provides a summary of the relevant standards dealing with both ITs and electrical substations, focusing on the possible temperature variation ranges. The goal of this brief review is to identify the realistic temperature ranges within which ITs can effectively operate.

### A. Standards on ITs

The relevant standard family dealing with ITs is the IEC 61869. Focusing on normal environmental conditions, the IEC 61869-1 [5] classified ITs into three different temperature categories, as reported in Table I.

Considering special environmental conditions, the same standard [5] identifies as preferred ranges of variation of temperature:

1) a) from −50 °C to +40 °C for very cold climates;
2) b) from −5 °C to +55 °C for very hot climates.

Considering the accuracy verification, the IEC 61869-1 [5] standard introduces the "temperature cycle accuracy test," which is required only for certain technologies like LPITs, but not for inductive ones. The test is performed by following a defined temperature profile that explores the entire range of variation of temperature identified by the IT temperature categories (Table I). During the test, the IT is supplied at rated frequency and with rated primary voltage or current only when the ambient temperature and maximum/minimum temperature are reached.

### B. Standard on Temperature Conditions in Electrical Substations

ITs are installed in locations covered by the IEC 60721 family standard [27], which classifies environmental conditions for electrical and electronic equipment. It defines categories for factors, such as temperature, humidity, and pressure, to establish design and construction standards ensuring safe and efficient operation in different environments.

For indoor cases, the specific standard to consider is IEC 60721-3-3 [28]. This standard identifies five environment classes, each with distinct temperature variation ranges, as outlined in Table II.

For outdoor cases, the specific standard to consider is IEC 60721-3-4 [29]. This standard identifies two main categories of locations (sheltered not wheatear protected and open-air) and five temperature classes, as reported in Table III.

It is important to note that there is a lack of uniformity between the temperature ranges defined for IT classes in [5]

TABLE II
TEMPERATURE CLASSES ACCORDING TO IEC 60721-3-3 STANDARD

| Class | Lowest temperature in °C | Highest temperature in °C | Description |
|---|---|---|---|
| 3K20 | +20 | +25 | Fully air-conditioned, enclosed places |
| 3K21 | +15 | +32 | Constantly tempered places |
| 3K22 | +5 | +40 | Tempered places |
| 3K23 | -5 | +55 | Enclosed places without temperature control |
| 3K24 | -25 | +55 | Places without temperature control |

TABLE III
TEMPERATURE CLASSES ACCORDING TO IEC 60721-3-4 STANDARD

| | Class | Lowest temperature in °C | Highest temperature in °C | Description |
|---|---|---|---|---|
| Sheltered | 4K23 | -45 | +70 | Tropical, arid, temperate and cold climatic type. |
| Sheltered | 4K24 | -50 | +70 | Polar climatic type. |
| Open air | 4K25 | +5 | +45 | Arid and temperate climatic classifications. |
| Open air | 4K26 | -20 | +50 | Tropical climatic classifications. |
| Open air | 4K27 | -50 | +45 | Cold and polar climatic classifications. |

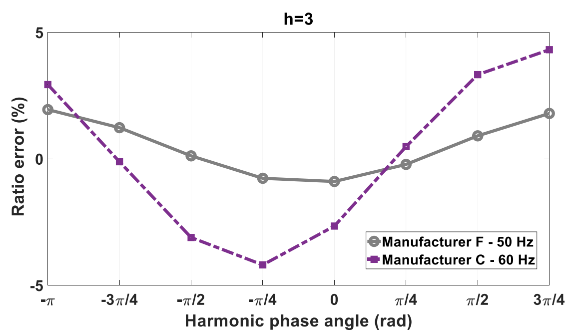


Fig. 1. Third harmonic ratio errors versus different harmonic displacements for two VTs from different manufacturers.

and those specified in IEC 60721-3, Parts 3 and 4 [28], [29] for environmental conditions for electrical and electronic equipment installation. This occurs even though the IEC 61869 -1 [5] standard explicitly references [28], [29] for detailed information on environmental condition classifications.

## III. VT NONLINEARITY: THEORETICAL BACKGROUND

Fig. 1 illustrates the third harmonic ratio error of two different VTs measured by supplying the VTs with a waveform consisting of the fundamental tone at their rated amplitude and frequency, along with a superimposed third harmonic at a reduced amplitude (1%) and varying the harmonic phase displacements relative to the fundamental tone. The result presented in Fig. 1 refers to tests performed under laboratory-controlled conditions, i.e., (23 °C ± 1 °C). As evident from the data in Fig. 1, different harmonics phase displacements result in different values of the third harmonic ratio errors, with a variability in the order of a percentage in the analyzed case.

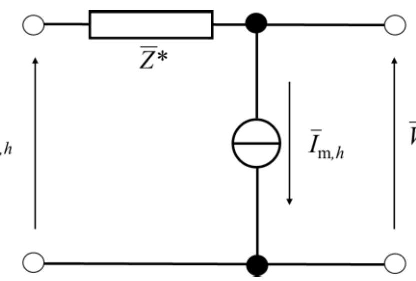


Fig. 2. VT simplified scheme to study the effect of nonlinearity.

This effect is due to the nonlinearity introduced by the magnetic characteristics of the VT iron core [17]. In fact, when a pure sinusoidal voltage is applied to the primary side of a VT, the hysteresis behavior of the magnetic core induces distortion in the magnetization current. By analyzing the harmonic content of the magnetization current, it includes harmonics, which are not present in the primary input signal.

Under no-load conditions, the behavior of a VT at a generic harmonic frequency (indicated as $h$) can be described using the simplified VT model depicted in Fig. 2, where:

1) $\overline{Z}^*$ represents the VT primary winding (the series connection of the equivalent resistance $R$ and the leakage inductance $L$).
2) The harmonic component of the magnetization current is modeled with the current generation $\overline{I}_{m,h}$.

The magnetization current depends on the hysteresis loop characteristics, determined by the peak and frequency of the input voltage. In realistic cases, the VT input voltage is composed of a large fundamental tone at rated amplitude with small superimposed harmonic, implying that it is possible to assume that the harmonic magnetization current depends only on the fundamental component.

Consequently, when a VT is energized with a sinusoidal voltage ("sin"), the harmonic secondary voltage can be expressed as follows:

$$\overline{V}^{\text{sin}}_{\text{s},h} = -\overline{Z}^* \cdot \overline{I}_{\text{m},h}. \tag{1}$$

Therefore, if the VT is supplied with a distorted voltage ("d") composed of a fundamental plus one harmonic tone, the harmonic tone at the VT secondary side will be the combination of the injected harmonic and the spurious one as described in the following equation:

$$\overline{V}^{\text{d}}_{\text{s},h} = \overline{V}^{\text{d}}_{\text{p},h} - \overline{Z}^* \cdot \overline{I}_{\text{m},h}. \tag{2}$$

Looking at (2), it is possible to say that $\overline{Z}^*$ is a constant parameter whereas, under realistic operating conditions, the magnetization current relies only on the fundamental component. Based on these observations, a compensation technique called SINDICOMP has been proposed and validated, as well detailed in [17]. Other technique with the same objective has been presented in [18] and [19] and compared to SINDICOMP [26]. In the study and analysis of this phenomenon and techniques, the effects of temperature have never been investigated as evident in (2), where this variable does not appear. However, scientific literature has highlighted that the magnetization processes in ferromagnetic materials are dependent on

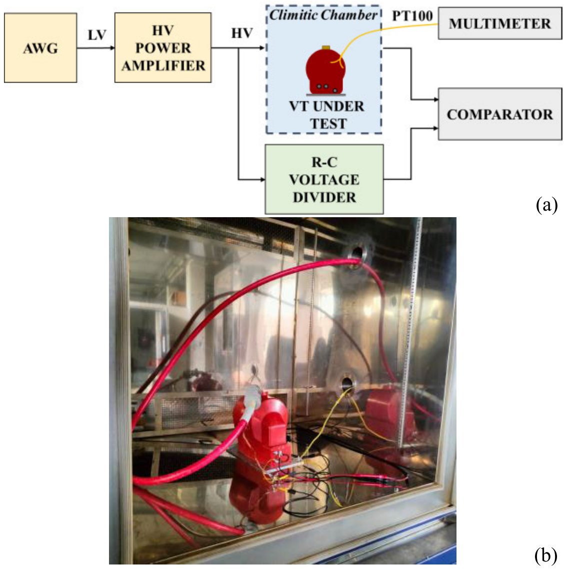


Fig. 3. Experimental setup. (a) Block scheme and (b) picture of the VT placed into the climatic chamber.

temperature [30], [31], [32]. Consequently, operating temperature can influence the VT magnetizing current, represented in Fig. 2 by the generator $\overline{I}_{m,h}$, and, in turn, affect the harmonic measurement errors introduced by the VT. Nevertheless, this issue has yet to be investigated, potentially leading to errors in assessing the harmonic accuracy of the VT and affecting the effectiveness of compensation techniques [26]. In fact, all the discussed methods include an identification step, where suitable lookup tables of compensation phasors are determined through tests performed in laboratory, under controlled conditions. These obtained lookup tables are subsequently used to compensate for harmonic measurements performed on-site, where temperatures and consequently the behavior of the VT may significantly vary.

## IV. Measurement Setup and Procedure

This section introduces the experimental setup used to assess the impact of temperature on the phenomenon of VT nonlinearity and the adopted test procedure.

### A. Generation and Measurement Setup

The general block scheme of the adopted generation and measurement setup is represented in Fig. 3, where also a picture of one the two VTs under test inside the climatic chamber is reported. The generation of distorted waveforms at megavolt level is obtained by using an arbitrary waveform generator (NI AWG 5421, 16 bit, ±12 V), coupled with a high-voltage power amplifier (Trek high-voltage power amplifier ±30 kV, ±20 mA from dc to 2.5 kHz at full voltage and to 30 kHz at reduced voltages). As regard the measurement, the reference transducer is a 30-kV wideband resistive–capacitive (*R*–*C*) voltage divider designed, built, and characterized at INRiM [33]. For the acquisition of the output voltages of the VT and the *R*–*C* divider, a comparator with various NI DAQ modules (from ±0.5 to ± 425 V, 24 bit, 50 kHz) is used.

To assess the impact of temperature variation on the VT nonlinearity, the device under test is placed inside a climatic chamber (100 × 100 × 120 $\text{cm}^3$, from −80 °C to +180 °C).

TABLE IV
Ratio Error Uncertainty Contributions From 5 to 20 kV and From 100 Hz up to 1 kHz

| Uncertainty Source | Standard Uncertainty (μV/V) |
|---|---|
| RCVD Calibration | 30 |
| Amplitude Dependence | 40 |
| Frequency response | 35 |
| Proximity effect | 21 |
| Stability | 10 |
| Acquisition system | 30 |
| **Relative expanded uncertainty** (Level of confidence 95%): **144 μV/V** | |

TABLE V
Phase Error Uncertainty Contributions From 5 to 20 kV and From 100 Hz up to 1 kHz

| Uncertainty Source | Standard Uncertainty (μrad) |
|---|---|
| RCVD Calibration | 30 |
| Amplitude Dependence | 16 |
| Frequency response | 140 |
| Proximity effect | 9 |
| Stability | 1 |
| Acquisition system | 30 |
| **Relative expanded uncertainty** (Level of confidence 95%): **295 μrad** | |

In order to monitor the temperature on the surface of the VT, a platinum resistance temperature detector (PT100) coupled with a digital multimeter (6.5 digit) is used.

The experimental measurement setup used in this study has been fully characterized at power frequency and within the frequency range of 100 Hz–1 kHz. At power frequency, the uncertainty (95% confidence level) is 70 $\mu$V/V and 70 $\mu$rad, determined through comparison with INRIM reference VTs. For the harmonic frequency range, the systematic ratio and phase errors, along with their associated uncertainties for the *R*–*C* divider, are determined using the following key procedures: 1) assessment of the voltage dependence of the scale factor (SF); 2) measurement of the frequency response at reduced amplitude; 3) stability tests; and 4) proximity tests.

The acquisition system is calibrated using a Fluke 5730 A calibrator. Detailed uncertainty budgets for ratio and phase errors from 100 Hz to 1 kHz are detailed in Tables IV and V.

### B. Test Procedure

To assess the impact of temperature on VTs accuracy in harmonics measurement, tests are performed by varying the climatic chamber temperature in [−25 °C, 55 °C] range that is the extreme temperature class (3K24) for the indoor case [28]. The climatic chamber is also configured to maintain a relative humidity level of 0%. Experimental tests are conducted after a waiting period that ranges from 10 to 40 h depending on the test temperature to achieve a thermal equilibrium.

Two different approaches can be used to evaluate the VTs dependence on temperature in relation to nonlinearity phenomenon. These approaches vary based on the test signal employed and the output performance index considered.

The first procedure involves supplying the VT with a sinewave as spectrally pure as possible at rated voltage and frequency (*sinusoidal test*). Even though the goal here is to generate a spectrally pure sinusoid, the frequency spectrum will inevitably contain spurious harmonic tones due to the nonideal behavior of the generation systems. The effect of temperature on the nonlinearity can be observed by comparing the injected spurious harmonics with those observed at the VT output for each temperature $T$, according to the following equation:

$$\Delta \bar{V}_h^{\sin}(T) = \bar{V}_{\mathrm{p},h}^{\sin}(T) - \bar{V}_{\mathrm{s},h}^{\sin}(T). \quad (3)$$

With the second approach, the VT is supplied with a test voltage composed of a fundamental tone plus 1 superimposed harmonic tone (*FH1 Test*), according to the following equation:

$$v_{\mathrm{FH1}}(t) = \sqrt{2}V_n \sin(2\pi f_0 t) + \sqrt{2}V_h \sin(2\pi h f_0 t + \varphi_h) \quad (4)$$

where $V_n$ and $f_0$ are the VT primary rated voltage and frequency, respectively; $V_h$, $h$, and $\varphi_h$ are the harmonic amplitude, order, and phase, respectively. Tests are performed by imposing the fundamental tone at rated conditions and the harmonic tone at $1\% \cdot V_n$ amplitude and varying both the order and phase shifts with the respect to the fundamental. Harmonic ratio and phase errors are then assessed based on the following equations:

$$\varepsilon_h = \frac{k_r V_{\mathrm{s},h} - V_{\mathrm{p},h}}{V_{\mathrm{p},h}} \quad (5)$$

$$\Delta\varphi_h = \varphi_{\mathrm{s},h} - \varphi_{\mathrm{p},h} \quad (6)$$

where $k_r = V_{\mathrm{p,r}}/V_{\mathrm{s,r}}$ is the rated transformation ratio ($V_{\mathrm{p,r}}$ and $V_{\mathrm{s,r}}$ are the rated primary and secondary voltages, respectively); $V_{\mathrm{s},h}$ and $V_{\mathrm{p},h}$ are the root mean square (rms) values of the primary and secondary $h$-order harmonic voltage, respectively; $\varphi_{\mathrm{p},h}$ and $\varphi_{\mathrm{s},h}$ are the phase angles of the primary and secondary $h$-order harmonic voltage, respectively.

Due to the nonlinearity phenomenon, the indices (5) and (6) assume different values for different harmonic phases $\varphi_h$ (see Fig. 1). For this reason, for each test temperature, two indices [see (7) and (8)] are properly defined to quantify the maximum errors introduced by the VT under test in the measurement of harmonics

$$\xi_h^T = \left|\varepsilon_h(T) - \bar{\varepsilon_h}(T)\right| \quad (7)$$

$$\Delta\Delta\psi_h^T = \left|\varphi_h(T) - \bar{\varphi_h}(T)\right| \quad (8)$$

where

1) $\cup\varphi_h$ indicates that the "maximum" function is computed over the entire range of the generated harmonic phase angle $\varphi_h$ at which ratio and phase errors are evaluated.
2) $\varepsilon_h(T)$ ($\Delta\varphi_h(T)$) is the ratio (phase) error at $h$-order harmonic, evaluated for different harmonic phase angles $\varphi_h$ at temperature T.
3) $\bar{\varepsilon_h}(T)$ ($\Delta\bar{\varphi_h}(T)$) is the mean value of the ratio (phase) error at $h$-order harmonic, evaluated for different harmonic phase angles $\varphi_h$ at temperature T.

TABLE VI
MAIN FEATURES OF THE VTS UNDER TEST

| VT | Primary Voltage (kV) | Secondary Voltage (V) | Accuracy Class | Temperature Category |
|---|---|---|---|---|
| $VT_I$ | 15/√3 | 100/√3 | 0.5 | -5/40 |
| $VT_O$ | 20/√3 | 100/√3 | 0.5 | -25/40 |

TABLE VII
MEAN VALUE OF THE VTS 3RD AND 5TH HARMONIC RATIO AND PHASE ERRORS IN THE INVESTIGATED TEMPERATURE RANGE

| | | -25 °C | -5 °C | 18 °C | 40 °C | 55 °C |
|---|---|---|---|---|---|---|
| $VT_I$ | $\bar{\varepsilon}_3$ (%) | -0.77 | -0.57 | 0.10 | 0.06 | 0.01 |
| | $\bar{\varepsilon}_5$ (%) | 1.27 | 0.68 | 0.06 | 0.05 | 0.02 |
| $VT_O$ | $\bar{\varepsilon}_3$ (%) | 0.47 | 0.46 | 0.40 | 0.40 | 0.47 |
| | $\bar{\varepsilon}_5$ (%) | 0.39 | 0.40 | 0.39 | 0.39 | 0.40 |

## V. EXPERIMENTAL RESULTS

The devices under test are two commercial resin insulated VTs from two different manufacturers, one is designed for indoor installation ($VT_I$) and one for the outdoor use ($VT_O$). The iron cores of the two VTs are made of grain-oriented iron-silicon alloy, and their main features are summarized in Table VI. For both the VTs, tests are performed under null burden condition.

As first analysis, considering the FH1 test, Table VII presents the mean values of the third and fifth harmonic ratio errors measured for the various generated harmonic phases $\varphi_h$. It can be observed that the two VTs exhibit different behaviors. Specifically, when considering $VT_I$, the mean values of the ratio errors observed within the investigated temperature range show a variation of 0.87% for the third harmonic and 1.20% for the fifth. On the contrary, for $VT_O$, the harmonic ratio errors remain relatively constant (variation in the order of hundreds of $\mu$V/V) across different temperatures.

As regard the behavior of the ratio and phase errors versus the generated harmonics, Figs. 4–7 present the results in terms of errors deviation with respect to the mean values. Each figure provides curves obtained at different temperatures.

First, it is observed that for various temperatures, the harmonic ratio and phase errors of both VTs assume different values, indicating an impact of temperature on the nonlinearity phenomenon. However, the indoor $VT_I$ shows a stronger dependency on temperature compared to $VT_O$.

In fact, focusing on the $VT_I$, it can be observed that with the decrease of the temperature, the errors notably increase exceeding 10% for the ratio error and one hundred of milliradians for the phase error. The indoor $VT_I$ is designed to operate from 40 °C down to −5 °C, in this temperature range variation of one order of magnitude are observed for the third harmonic ratio error: $\xi_3^{-5\ °\mathrm{C}}$ has a value of 8.8%, $\xi_3^{18\ °\mathrm{C}}$ is equal to 0.62%, whereas at 40 °C, $\xi_3^{40\ °\mathrm{C}}$ decreases to 0.15%. Including into the analysis also the other test temperatures, the trend is confirmed being $\xi_3^{55\ °\mathrm{C}} = 0.07\%$ and $\xi_3^{-25\ °\mathrm{C}} = 14.18\%$. Similar results are also observed for other harmonics and for phase errors. For instance, $\psi_5^{-25\ °\mathrm{C}} = 132.2$ mrad, whereas $\psi_5^{55\ °\mathrm{C}}$ is equal to 1.5 mrad.

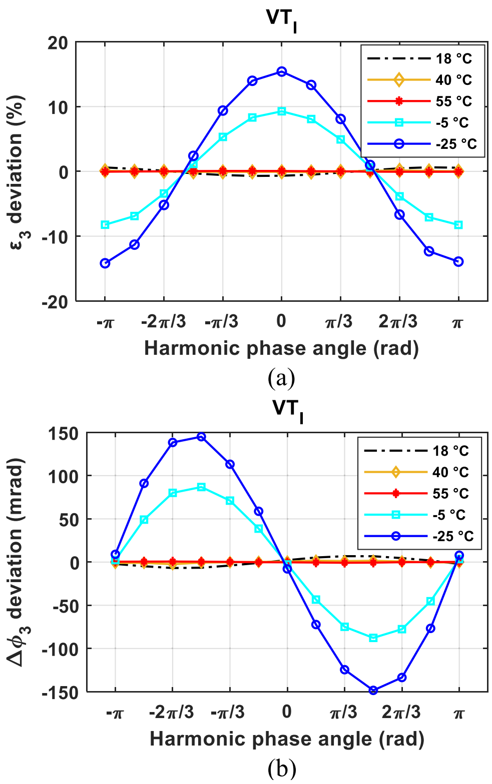


Fig. 4. $VT_I$ third harmonic ratio (a) and phase (b) errors measured at different temperatures: 18 °C (dashed-dotted line), 40 °C (diamond marker), 55 °C (asterisk marker), −5 °C (square marker), and −25 °C (circle marker).

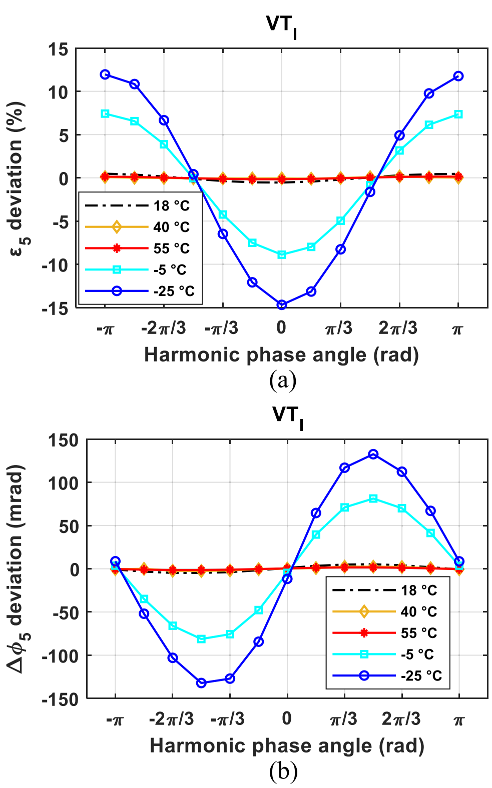


Fig. 5. $VT_I$ fifth harmonic ratio (a) and phase (b) errors measured at different temperatures: 18 °C (dashed-dotted line), 40 °C (diamond marker), 55 °C (asterisk marker), −5 °C (square marker), and −25 °C (circle marker).

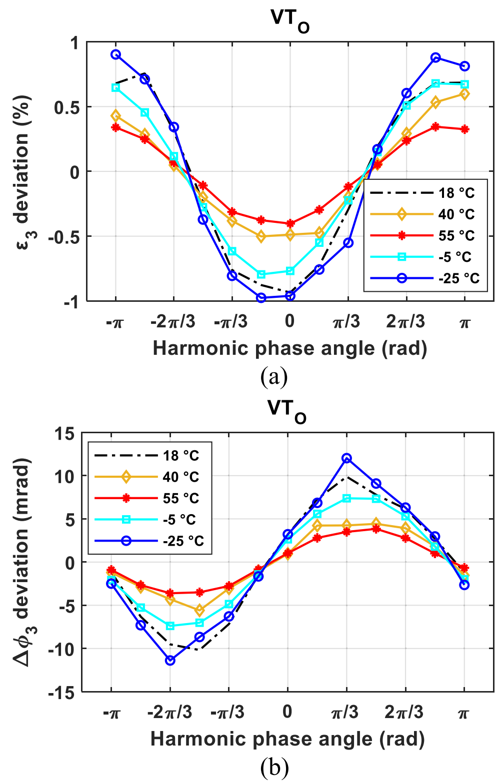


Fig. 6. $VT_O$ third harmonic ratio (a) and phase (b) errors measured at different temperatures: 18 °C (dashed-dotted line), 40 °C (diamond marker), 55 °C (asterisk marker), −5 °C (square marker), and −25 °C (circle marker).

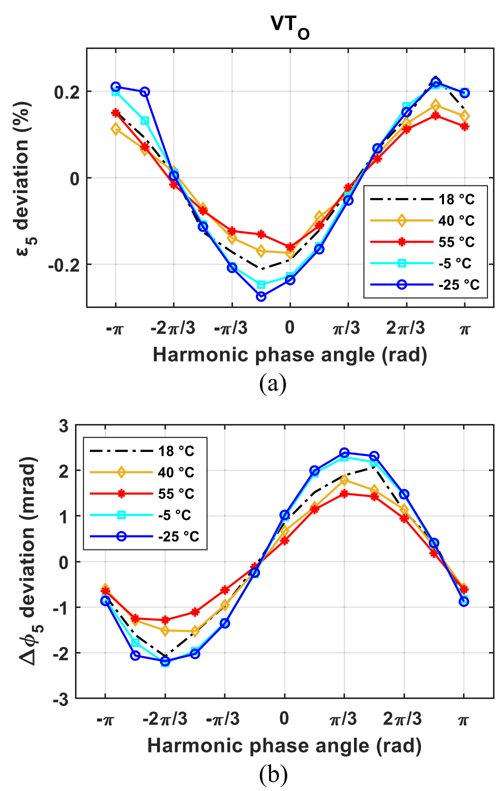


Fig. 7. $VT_O$ fifth harmonic ratio (a) and phase (b) errors measured at different temperatures: 18 °C (dashed-dotted line), 40 °C (diamond marker), 55 °C (asterisk marker), −5 °C (square marker), and −25 °C (circle marker).

Regarding the outdoor $VT_O$, its operational temperature range spans from −25 °C to 40 °C. As evidenced in Figs. 6 and 7, the deviations in harmonic ratio and phase errors are notably lower compared to those observed for

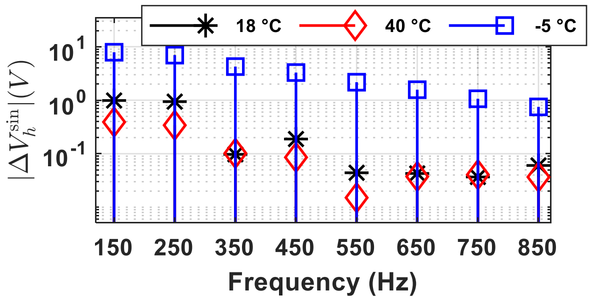


Fig. 8. $VT_I$ amplitude of the spurious harmonic tones measured under a sinewave at rated conditions at different operating temperatures: 18 °C (asterisk marker), 40 °C (diamond marker), and −5 °C (square marker).

$VT_I$. Examining the third harmonic ratio error, the measured values are as follows: $\xi_3^{-25\ ^\circ C} = 0.91\%$, $\xi_3^{-5\ ^\circ C} = 0.68\%$, $\xi_3^{18\ ^\circ C} = 0.75\%$, $\xi_3^{40\ ^\circ C} = 0.60\%$, and $\xi_3^{55\ ^\circ C} = 0.35\%$. Thus, the variations across the investigated temperature range are limited within a factor of 3. Similarly, for the third harmonic phase error, the curve deviations remain within a factor of 3, with the respective values: $\psi_3^{-25\ ^\circ C} = 11.6$ mrad, $\psi_3^{-5\ ^\circ C} = 7.4$ mrad, $\psi_3^{18\ ^\circ C} = 10.2$ mrad, $\psi_3^{40\ ^\circ C} = 5.6$ mrad, and $\psi_3^{55\ ^\circ C} = 3.8$ mrad.

For a comprehensive understanding over a wider frequency range, Fig. 8 illustrates the magnitude of the harmonic spurious phasors, as determined by (3), obtained suppling $VT_I$ with a sinusoidal waveform (THD $\leq 0.02\%$) at rated voltage at three distinct temperatures. This analysis focuses only on $VT_I$ due to its higher sensitivity to temperature compared to $VT_O$. As can be observed in Fig. 8, even if $VT_I$ belongs to −5/40 °C class, different scenarios are observed in terms of nonlinearity within this temperature range. In fact, when operating at −5 °C, the amplitudes of $\Delta \bar{V}_h^{\sin}$ are more than 20 times higher than those measured at 40 °C over the entire considered frequency range that goes from 150 Hz to 850 kHz.

Moreover, the experimental results obtained under controlled laboratory temperature and presented in literature, as outlined in [26], prove that nonlinearity is a frequency-dependent phenomenon, becoming negligible beyond the 10–15th harmonic. Nevertheless, as illustrated in Fig. 8, experiments on $VT_I$ have demonstrated that it is not correct to confine nonlinearity to the first 15 harmonics. Depending on the operating temperature, spurious harmonics may be nonnegligible even at higher frequencies. For instance, considering as threshold $\Delta \bar{V}_h^{\sin} \leq 0.1$ V, at $T = 40$ °C, the spurious phasors remain below 0.1 V from the 7th harmonic, while at $T = 18$ °C, this threshold is reached from the 11th harmonic. When $VT_I$ operates at $T = -5$ °C, spurious phasors are below 0.1 V only after the 31th harmonic.

Moreover, the experimental results obtained under controlled laboratory temperature and presented in literature, as outlined in [26], prove that nonlinearity is a frequency-dependent phenomenon, becoming negligible beyond the 10–15th harmonic. Nevertheless, as illustrated in Fig. 8, experiments on $VT_I$ have demonstrated that it is not correct to confine nonlinearity to the first 15 harmonics. Depending on the operating temperature, spurious harmonics may be nonnegligible even at higher frequencies. For instance, considering as threshold $\Delta \bar{V}_h^{\sin} \leq 0.1$ V, at $T = 40$ °C, the spurious phasors remain below 0.1 V from the 7th harmonic, while at $T = 18$ °C, this threshold is reached from the 11th harmonic. When $VT_I$ operates at $T = -5$ °C, spurious phasors are below 0.1 V only after the 31th harmonic.

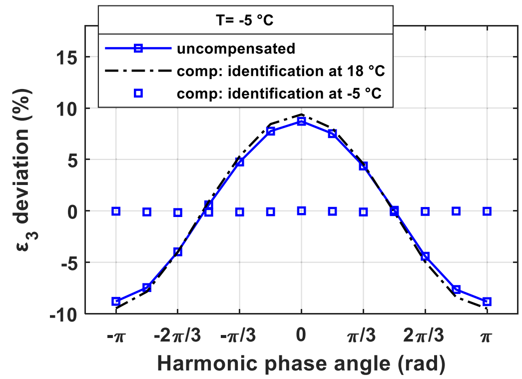


Fig. 9. Third harmonic ratio error of the VTI with a fundamental component at 100% and a third harmonic at 1%, measured at −5 °C. Results are shown without compensation (solid line with square markers), with SINDICOMP applied using a lookup table obtained at 18 °C (dotted line), and with SINDICOMP applied using a lookup table obtained at −5 °C (square markers without a line).

## VI. Results Discussion and Final Considerations

The experimental test results presented in the previous Section V have revealed an important dependency of the VTs harmonic errors due to the nonlinearity phenomenon on the temperature. In particular, as the temperature increases, a reduction in the variation of the harmonics ratio and phase error curves is evident for both tested VTs, with near-flat curves observed at 55 °C for $VT_I$ ($\xi_3^{55\ ^\circ C} = 0.07\%$ and $\psi_3^{55\ ^\circ C} = 0.63$ mrad). On the contrary, at lower temperatures, different scenarios occur between the two devices and for the $VT_I$ also −5 °C, which is an admissible operating temperature (see Table VI), represents a critical condition in terms of harmonic accuracy. Considering the IEC 61869-1 v2 standard [5], which defines accuracy across five frequency ranges (WB0 to WB4), the $VT_I$ may either stay within or exceed the limits set for the WB0 range (±5% for a 0.5 accuracy class), depending on its temperature. As regard $VT_O$, it meets the requirement of the IEC 61869-1 standard [5] for the WB0 class at every investigated temperature.

The different sensitivity of the two VTs with respect to the temperature can be attributed to the fact that they are constructed differently. Regarding the insulating material, the indoor VT is insulated exclusively with epoxy resin, while the outdoor VT is insulated with both epoxy resin and silicone. Additionally, the ferromagnetic core is sized differently; specifically, outdoor VT is built with cores containing a significantly greater amount of iron (one-third more).

As additional comment, the experimental findings presented in Section V suggest the necessity of studying an improved version of the nonlinearity compensation techniques [26] to include the temperature of the VT as an additional input parameter when VTs are used in premises other than 3K20. In this regard, a preliminary study is presented in Fig. 9, where the results obtained using the SINDICOMP technique, as described in Section III, are shown. As can be seen, employing the lookup table obtained at 18 °C for compensating nonlinearity error of $VT_I$ operating at −5 °C yields no correction. On the contrary, using the lookup table acquired at the actual operating temperature significantly reduces the nonlinearity error and $\xi_3^{-5\ ^\circ\mathrm{C}}$ goes from 8.8% to 0.16%.

## VII. Conclusion

This article has investigated the impact of temperature on the performance of VTs in harmonic measurements. Specifically, the study focused on the influence of temperature on the nonlinearities introduced by the $B$–$H$ characteristic of the VT iron core. A preliminary analysis of the international standards dealing with both VTs and the premises for their installation was conducted to identify a realistic temperature variation range to adopt for the experimental activity. The INRiM reference generation and measurement setup was modified to include a climatic chamber and it was used to test two VTs designed for different installations (indoor and outdoor).

Results showed that the nonlinearity phenomenon can be highly sensitive to temperature. In particular, errors introduced in the harmonic measurement can vary within a wide range, from hundreds of ppm to tens of percentage, depending on the VT temperature. The experimental results emphasize the importance of incorporating the temperature of the VT as an additional input parameter in the existing compensation techniques. This underscores the need for additional studies on these methods to ensure their effectiveness in realistic environmental conditions.

## References


[1] C. Fetting, "The European green deal," ESDN Office, Vienna, Austria, Tech. Rep. 2, Dec. 2020.

[2] *European Commission, Directorate-General for Communication, REPowerEU, Joint European Action for More Affordable, Secure and Sustainable Energy*, Publications Office Eur. Union, Brussels, Belgium, 2022, doi: 10.2775/076377.

[3] X. Liang, "Emerging power quality challenges due to integration of renewable energy sources," *IEEE Trans. Ind. Appl.*, vol. 53, no. 2, pp. 855–866, Mar./Apr. 2017.

[4] L. Peretto, "The role of measurements in the smart grid era," *IEEE Instrum. Meas. Mag.*, vol. 13, no. 3, pp. 22–25, Jun. 2010, doi: 10.1109/MIM.2010.5475163.

[5] *Instrument Transformers—Part 1: General Requirements*, Standard IEC 61869-1, Jun. 2023.

[6] *Instrument Transformers—Part 2: Additional Requirements for Inductive Curret Transformers*, Standard IEC 61869-2, 2011.

[7] *Instrument Transformers-Part 3: Additional Requirements for Inductive Voltage Transformers*, Standard IEC, 61869-3, 2011.

[8] M. Kaczmarek and R. Nowicz, "Application of instrument transformers in power quality assessment," in *Proc. Modern Electric Power Syst.*, Wroclaw, Poland, Sep. 2010, pp. 1–5.

[9] K. Draxler and R. Styblikova, "Using instrument transformers in a wider frequency range," in *Proc. IEEE Int. Instrum. Meas. Technol. Conf.*, Hangzhou, China, May 2011, pp. 1–4, doi: 10.1109/IMTC.2011.5944298.

[10] M. Kaczmarek and E. Stano, "Proposal for extension of routine tests of the inductive current transformers to evaluation of transformation accuracy of higher harmonics," *Int. J. Electr. Power Energy Syst.*, vol. 113, pp. 842–849, Dec. 2019, doi: 10.1016/j.ijepes.2019.06.034.

[11] M. Kaczmarek and E. Stano "Review of measuring methods, setups and conditions for evaluation of the inductive instrument transformers accuracy for transformation of distorted waveforms," *Energies*, vol. 16, p. 4360, May 2023, doi: 10.3390/en16114360.

[12] G. Crotti et al., "Instrument transformers for power quality measurements: A review of literature and standards," in *Proc. IEEE 11th Int. Workshop Appl. Meas. Power Syst. (AMPS)*, Cagliari, Italy, Sep. 2021, pp. 1–6, doi: 10.1109/AMPS50177.2021.9586028.

[13] R. Stiegler, J. Meyer, J. Kilter, and S. Konzelmann, "Assessment of voltage instrument transformers accuracy for harmonic measurements in transmission systems," in *Proc. 17th Int. Conf. Harmon. Quality Power (ICHQP)*, Belo Horizonte, Brazil, Oct. 2016, pp. 152–157, doi: 10.1109/ICHQP.2016.7783472.

[14] I. Jayathilaka et al., "Calibration system for high-voltage transformers with multiharmonic distorted waveforms," *IEEE Trans. Instrum. Meas.*, vol. 73, pp. 1–13, 2024, doi: 10.1109/TIM.2024.3370744.

[15] C. Buchhagen, M. Fischer, L. Hofmann, and H. Däumling, "Metrological determination of the frequency response of inductive voltage transformers up to 20 kHz," in *Proc. IEEE Power Energy Soc. Gen. Meeting*, Vancouver, BC, Canada, Jul. 2013, pp. 1–5, doi: 10.1109/PESMG.2013.6672835.

[16] M. Agazar et al., "Power grids and instrument transformers up to 150 kHz: A review of literature and standards," *Sensors*, vol. 24, no. 13, p. 4148, Jun. 2024, doi: 10.3390/s24134148.

[17] A. Cataliotti et al., "Compensation of nonlinearity of voltage and current instrument transformers," *IEEE Trans. Instrum. Meas.*, vol. 68, no. 5, pp. 1322–1332, May 2019, doi: 10.1109/TIM.2018.2880060.

[18] M. Kaczmarek and E. Stano, "Nonlinearity of magnetic core in evaluation of current and phase errors of transformation of higher harmonics of distorted current by inductive current transformers," *IEEE Access*, vol. 8, pp. 118885–118898, 2020, doi: 10.1109/ACCESS.2020.3005331.

[19] S. Toscani, M. Faifer, A. Ferrero, C. Laurano, R. Ottoboni, and M. Zanoni, "Compensating nonlinearities in voltage transformers for enhanced harmonic measurements: The simplified Volterra approach," *IEEE Trans. Power Del.*, vol. 36, no. 1, pp. 362–370, Feb. 2021, doi: 10.1109/TPWRD.2020.2978668.

[20] S. Zhao, H. Y. Li, P. Crossley, and F. Ghassemi, "Testing and modelling of voltage transformer for high order harmonic measurement," in *Proc. 4th Int. Conf. Electric Utility Deregulation Restructuring Power Technol. (DRPT)*, Weihai, China, Jul. 2011, pp. 229–233, doi: 10.1109/DRPT.2011.5993894.

[21] M. Klatt, J. Meyer, M. Elst, and P. Schegner, "Frequency responses of MV voltage transformers in the range of 50 Hz to 10 kHz," in *Proc. 14th Int. Conf. Harmon. Quality Power*, Bergamo, Italy, Sep. 2010, pp. 1–6, doi: 10.1109/ICHQP.2010.5625484.

[22] R. Stiegler, J. Meyer, and P. Schegner, "Portable measurement system for the frequency response of voltage transformers," in *Proc. IEEE Int. Conf. Harmon. Quality Power*, Jun. 2012, pp. 745–750.

[23] R. Stiegler and J. Meyer, "Impact of external influences on the frequency dependent transfer ratio of resin cast MV voltage instrument transformers," in *Proc. 20th Int. Conf. Harmon. Quality Power (ICHQP)*, Naples, Italy, May 2022, pp. 1–6, doi: 10.1109/ICHQP53011.2022.9808776.

[24] M. Agazar, D. Istrate, and P. Pradayrol, "Evaluation of the accuracy and frequency response of medium-voltage instrument transformers under the combined influence factors of temperature and vibration," *Energies*, vol. 16, no. 13, p. 5012, Jun. 2023, doi: 10.3390/en16135012.

[25] P. S. Letizia et al., "Characterization of instrument transformers under realistic conditions: Impact of single and combined influence quantities on their wideband behavior," *Sensors*, vol. 23, no. 18, p. 7833, Sep. 2023, doi: 10.3390/s23187833.

[26] G. D'Avanzo et al., "Theory and experimental validation of two techniques for compensating VT nonlinearities," *IEEE Trans. Instrum. Meas.*, vol. 71, pp. 1–12, 2022, doi: 10.1109/TIM.2022.3147883.

[27] *Classification of Environmental Conditions—Part 1: Environmental Parameters and Their Severities*, Standard IEC, 60721-1, 1990.

[28] *Classification of Environmental Conditions—Part 3–3: Classification of Groups of Environmental Parameters and Their Severities—Stationary Use at Weatherprotected Locations*, Standard IEC 60721-3-3, 2019.

[29] *Classification of Environmental Conditions—Part 3–4: Classification of Groups of Environmental Parameters and Their Severities—Stationary Use at Not-Weatherprotected Locations*, Standard IEC 60721-3-4, 2019.

[30] A. Raghunathan, Y. Melikhov, J. E. Snyder, and D. C. Jiles, "Theoretical model of temperature dependence of hysteresis based on mean field theory," *IEEE Trans. Magn.*, vol. 46, no. 6, pp. 1507–1510, Jun. 2010, doi: 10.1109/TMAG.2010.2045351.

[31] C. W. Chen, "Temperature dependence of magnetic properties of silicon-iron," *J. Appl. Phys.*, vol. 29, no. 9, pp. 1337–1343, 1958, doi: 10.1063/1.1723438.

[32] C. Steinmetz, "On the law of hysteresis," *Proc. IEEE*, vol. 72, no. 2, pp. 197–221, Feb. 1984, doi: 10.1109/PROC.1984.12842.

[33] G. Crotti et al., "Frequency compliance of MV voltage sensors for smart grid application," *IEEE Sensors J.*, vol. 17, no. 23, pp. 7621–7629, Dec. 2017, doi: 10.1109/JSEN.2017.2726116.

**Palma Sara Letizia** received the M.Sc. degree (summa cum laude) in power electronic engineering from the University of Campania "Luigi Vanvitelli," Aversa, Italy, in 2018, and the Ph.D. degree in metrology from the Politecnico di Torino, Turin, Italy, in 2022.

Since 2022, she has been a Researcher at the Istituto Nazionale di Ricerca Metrologica (INRIM), Turin. Her main scientific interests lie in metrology applied to power grids, particularly in the development of new procedures and reference sensors for power quality and phasor measurement unit applications.

**Gabriella Crotti** received the degree (cum laude) in physics from the University of Torino, Turin, Italy, in 1986.

Since then, she has been with the Istituto Nazionale di Ricerca Metrologica (INRIM), Turin, where she presently works as the Director Technologist of the Electric and electromagnetic Field and System Sector. She was the Leader of the EMPIR project 19NRM05 IT4PQ. Her research interests are focused on the development and characterization of references and techniques for voltage and current measurements in high- and medium-voltage grids and on the traceability of electric and magnetic field measurements at low and intermediate frequency.

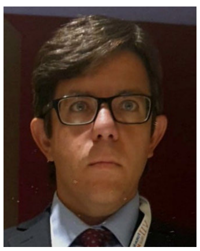

**Antonio Delle Femine** (Member, IEEE) received the M.Sc. degree (summa cum laude) in electronic engineering and the Ph.D. degree in electrical energy conversion from the University of Campania, Aversa, Italy, in 2005 and 2008, respectively.

From 2008 to 2017, he was a freelancer with many national and international companies. He worked as a Software and Hardware Engineer (Ditron S.r.l., Italy) and Senior Embedded Firmware Engineer (G-LAB gmbH, Switzerland). He was involved in the design of many products for both industrial and consumer electronics: he worked on fleet monitoring, thermal printers, electronic scales and cash registers, distributed monitoring systems for PV plants, Hi-Fi radios and home appliances, automatic end-of-line testing, augmented reality devices, and radioactivity measurement instrumentation (in collaboration with the Institute of Nuclear Physics, INFN, Naples, Italy). Since 2018, he has been a Researcher with the University of Campania. His main scientific interests are the power measurement theory, the design, implementation and characterization of digital-measurement instrumentation and automatic measurement systems, radioactivity measurements, wearable sensors, and physiological measurements.

Dr. Femine is a member of the IEEE Instrumentation and Measurement Society.

**Daniele Gallo** (Member, IEEE) received the Laurea degree in electronic engineering and the Ph.D. degree in electrical energy conversion from the University of Campania "Luigi Vanvitelli" (formerly Second University of Naples), Aversa, Italy, in 1999 and 2003, respectively.

He is currently a Full Professor with the University of Campania "Luigi Vanvitelli." He was the author of numerous scientific papers and had the responsibility of different research projects. His main scientific interests are: dc and ac power quality analysis; power and energy measurement in nonsinusoidal conditions; design, implementation, and characterization of measurement systems for electrical power system; design and implementation of smart meter for smart grid application; and electrical transducer characterization.

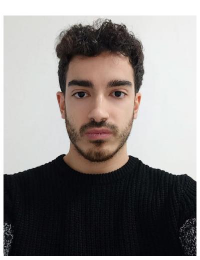

**Claudio Iodice** (Student Member, IEEE) was born in Naples, Italy, in 1997. He received the M.Sc. degree (summa cum laude) in aerospace engineering from the University of Campania "Luigi Vanvitelli," Aversa, Italy, in 2022, where he is currently pursuing the Ph.D. degree in energy conversion.

His main scientific interests are the calibration of instrument transformers, measurement systems for e-mobility, and control and optimization algorithms for aerospace applications.

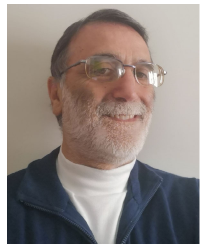

**Carmine Landi** (Senior Member, IEEE) was born in Salerno, Italy, in 1955. He received the Laurea degree in electrical engineering from the University of Naples, Naples, Italy, in 1981.

He was an Assistant Professor of electrical measurement from the University of Naples "Federico II," Naples, from 1982 to 1992. He was an Associate Professor in electrical and electronic measurements at the University of L'Aquila, L'Aquila, Italy, from 1992 to 1999. He has been a Full Professor at the University of Campania "Luigi Vanvitelli" (formerly Second University of Naples), Aversa, Italy, since 1999. He has authored almost 200 international papers in the field of real-time measurement apparatus, automated test equipment, high-precision power measurement, and power quality measurement. His main scientific interests are related to the setup of digital measurement instrumentation, the automatic testing of electrical machines, such as asynchronous motors and power transformers, measurement techniques for the characterization of digital communication devices, and the use of digital signal processors for real-time measurements.

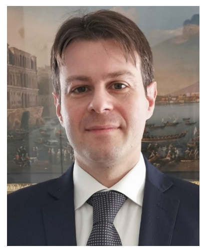

**Mario Luiso** (Member, IEEE) was born in Naples, Italy, on July 6, 1981. He received the Laurea degree (summa cum laude) in electronic engineering and the Ph.D. degree in electrical energy conversion from the University of Campania "Luigi Vanvitelli," Aversa, Italy, in 2005 and 2007, respectively.

He is currently an Associate Professor with the Department Engineering, University of Campania "Luigi Vanvitelli." He is the author and co-author of more than 200 papers published in books, scientific journals, and conference proceedings. His main scientific interests are related to the development of innovative methods, sensors and instrumentation for power system measurements, in particular power quality, calibration of instrument transformers, phasor measurement units, and smart meters.

Dr. Luiso is a member of IEEE Instrumentation and Measurement Society.

**Davide Signorino** was born in Naples, Italy, in 1990. He received the Laurea degree in electronic engineering from the University of Campania Luigi Vanvitelli, Avera, Italy, in 2018, with a specialization in power electronics, and the Ph.D. degree in metrology from the Politecnico di Torino, Turin, Italy, in 2022.

Since 2022, he has been a Researcher at the Istituto Nazionale di Ricerca Metrologica (INRIM), Turin. His current research topic is the metrology applied to the railway systems, particularly for the power quality and energy exchange between the supply line and train analyses, calibration of energy meters, and characterization of voltage and current transducers.

**Domenico Giordano** (Member, IEEE) received the Ph.D. degree in electrical engineering from the Politecnico di Torino, Turin, Italy, in May 2007.

Since December 1, 2010, he has been a Researcher, permanent position with the Quality of Life Division, Istituto Nazionale di Ricerca Metrologica (INRIM), Turin. He is currently coordinating the European EPM project 22NRM04 e-TRENY. His research activities are focused on the development and characterization of systems and voltage/current transducers for calibration and power quality measurements on medium-voltage grids and on railway supply systems, on the calibration of energy meters for onboard train installation, and on the study of ferroresonance phenomena. Moreover, he is involved in the development of generation and measurement systems of electromagnetic fields for calibration and dosimetric purposes.